



Drastic enhancement of d -wave superconductivity in an extended checkerboard Hubbard modelKai Cheng ¹, Shi-Chao Fang,² and Zhong-Bing Huang ^{1,*}¹*School of Physics, Hubei University, Wuhan 430062, China*²*School of Mathematics and Physics, Nanyang Institute of Technology, Nanyang 473004, China*

(Received 7 September 2023; revised 11 December 2023; accepted 12 January 2024; published 31 January 2024)

Motivated by the recent discovery of anomalously strong nearest-neighbor attraction in the one-dimensional hole-doped cuprate $\text{Ba}_{2+x}\text{Sr}_x\text{CuO}_{3+\delta}$, we investigate the d -wave superconducting property of an extended checkerboard Hubbard model, which includes an intraplaquette nearest-neighbor attraction V . Our quantum Monte Carlo simulations reveal that, for small interplaquette hopping integral t' , V induces a drastic enhancement of long-range d -wave pairing correlations in the parameter range of $0.0 \leq U \leq 6.0t$ (t is the intraplaquette hopping integral) when the electron density lies between half-filling and quarter-filling. At $V = -0.4t$, one order of magnitude larger d -wave pairing correlations are observed compared to the ones at $V = 0.0t$ and, more importantly, they exceed the values of the free electron system, signifying the existence of d -wave superconductivity. The exact diagonalization calculations on the 2×2 plaquette indicate that the enhancement of d -wave pairing correlations can be attributed to the V -induced enhancement of pair-binding energy. Our findings provide a new perspective on the realization of high-temperature d -wave superconductivity via the combination of nearest-neighbor attraction and electronic inhomogeneity.

DOI: [10.1103/PhysRevB.109.014519](https://doi.org/10.1103/PhysRevB.109.014519)**I. INTRODUCTION**

Exploring the superconducting (SC) mechanism of cuprate high-temperature superconductors has been a central research topic in the condensed matter physics community [1–9]. After more than three decades of intensive research, numerous experiments have demonstrated that the cuprate superconductors have an anisotropic d -wave SC symmetry [10–13] and that the medium of SC electron pairs may be antiferromagnetic spin fluctuations [14–16]. Early theoretical studies based on single- and multi-band correlated electron models [17–31] have made significant progresses, but no consensus has been reached so far on the high-temperature SC mechanism. Recent angle-resolved photoemission spectroscopy revealed the evolution of holon and spinon energy bands with doping density in the one-dimensional cuprate $\text{Ba}_{2+x}\text{Sr}_x\text{CuO}_{3+\delta}$ [32]. A comparison with the theory indicated that the holon folding branch matches perfectly with the result predicted by the one-dimensional Hubbard model with strong nearest-neighbor (NN) attraction. Such an attraction can be mediated by electron-phonon coupling [33,34]. Considering the structure similarity among cuprates, the two-dimensional extended Hubbard model with NN attractive interaction is regarded as a suitable model to understand d -wave superconductivity in cuprates.

Up to now, a number of theoretical attempts [35–45] have been made to investigate the SC property of the t - U - V extended Hubbard model. The presence of V -induced d -wave superconductivity in the weak correlation regime ($U < 2t$) has been well established with the aid of analytic analyses

[35,36] and numerical simulations [37,38]. Yet it remains unclear on the role of NN attraction in the intermediate and strong correlation regimes. A recent density matrix renormalization group study of the extended Hubbard model on four-leg square cylinders showed that the NN electron attraction can notably enhance the long-distance SC correlations while simultaneously suppressing the charge-density-wave correlations [39]. In addition, dynamic cluster calculations of the extended Hubbard model on the 2×2 cluster indicated that the NN attraction enhances antiferromagnetic spin fluctuations but enhances (suppresses) the charge fluctuations for small (large) momentum transfer, leading to 10–15% enhancement of d -wave superconductivity [40]. On the other hand, quantum Monte Carlo simulations of the extended Hubbard model on two-dimensional finite-size lattices [41,46] showed that the NN attraction produces a significant enhancement of short-range d -wave pairing correlations, but little effect on the long-range d -wave pairing correlations, suggesting that d -wave superconductivity is hardly affected by the NN attraction.

Besides NN attraction, the effect of inhomogeneity on the high-temperature SC mechanism has received widespread attention [47–56]. The checkerboard Hubbard model with inhomogeneous hopping integral was reported to harbor a rich variety of phases such as d -wave Mott insulator and d -wave superconductivity, depending on the magnitude of U and electron filling [47]. However, whether inhomogeneity supports d -wave superconductivity has not yet reached a clear conclusion. Both positive [48–52] and negative [53–56] results have been reported based on different numerical methods. Motivated by the above experimental and theoretical research, we investigate the effects of NN attraction and inhomogeneity on the d -wave SC property by analyzing an extended

*huangzb@hubu.edu.cn

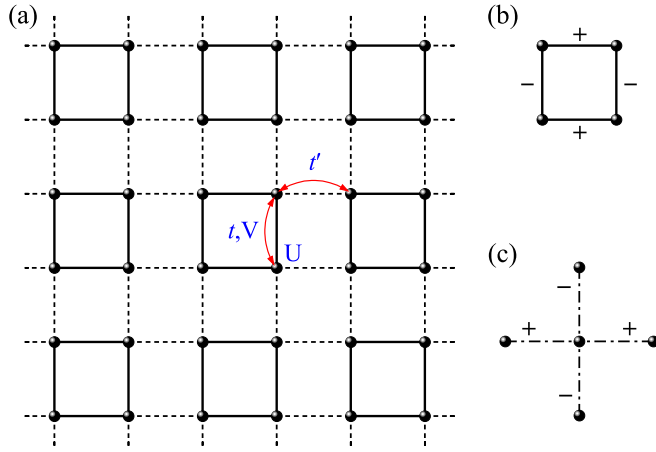


FIG. 1. (a) Sketch of the checkerboard lattice. The solid and dashed lines stand for the intraplaquette and interplaquette bonds on the square lattice, respectively. (b) Cluster d -wave pairing and (c) conventional d -wave pairing. “+” and “-” represent the form factors. The dash-dotted lines refer to either solid or dashed lines on the checkerboard lattice.

checkerboard Hubbard model with intraplaquette NN attraction. The constrained-path quantum Monte Carlo (CPQMC) [57–60] and exact diagonalization (ED) are employed to simulate the correlated electron system. Our CPQMC results reveal that the NN attraction induces a drastic enhancement of d -wave superconductivity in the presence of strong inhomogeneity. ED calculations indicate that the enhanced d -wave superconductivity originates from the enhancement of pair binding energy.

This paper is organized as follows. In Sec. II, we introduce the extended checkerboard Hubbard model and the CPQMC method. Section III contains our calculation results and discussion. Finally, we present the summary and prospect of this paper.

II. MODEL AND METHOD

As shown Fig. 1(a), the checkerboard lattice consists of periodically arranged 2×2 plaquettes. The solid and dashed lines represent the intraplaquette and interplaquette bonds, respectively. The extended Hubbard model on the checkerboard lattice is defined as

$$H = -t \sum_{\langle i, j \rangle, \sigma} (c_{i, \sigma}^\dagger c_{j, \sigma} + \text{H.c.}) - t' \sum_{\langle i, j \rangle', \sigma} (c_{i, \sigma}^\dagger c_{j, \sigma} + \text{H.c.}) + U \sum_i n_{i, \uparrow} n_{i, \downarrow} + V \sum_{(i, j), \sigma, \sigma'} n_{i, \sigma} n_{j, \sigma'}, \quad (1)$$

Here, $\langle i, j \rangle$ and $\langle i, j \rangle'$ denote the restriction of the summation to NN sites within and between plaquettes, respectively. $c_{i, \sigma}^\dagger$ ($c_{i, \sigma}$) is the creation (annihilation) operator on site i with spin σ and $n_{i, \sigma} = c_{i, \sigma}^\dagger c_{i, \sigma}$ is the number operator on site i . t (t') represents the intraplaquette (interplaquette) hopping integral. $t'/t < 1$ corresponds to the inhomogeneous case, and $t'/t = 1$ to the homogeneous case. U and V denote the on-site Coulomb repulsion and the NN attractive interaction within the same plaquette.

The Hamiltonian in Eq. (1) is simulated by a sign-problem-free auxiliary-field quantum Monte Carlo, i.e., the CPQMC method, which projects out the ground state from a trial wave function by a branching random walk in an overcomplete space of constrained Slater determinants, having positive overlaps with a known Slater determinant. More specifically, starting with a certain trial wave function $|\Psi_T\rangle$, we project out the ground state by iterating

$$|\Psi^{(n+1)}\rangle = e^{-\Delta\tau\hat{H}}|\Psi^{(n)}\rangle, \quad (2)$$

where $|\Psi^{(0)}\rangle = |\Psi_T\rangle$ and $\Delta\tau$ is a small positive parameter. Extensive benchmark calculations demonstrated that the systematic error induced by constraint is within a few percent and the physical observables are insensitive to the choice of trial wave function [57–60]. A benchmark study of the CPQMC method is presented in Appendix A. In our CPQMC simulations, we employ closed-shell electron fillings and use the corresponding free electron wave function as the trial wave function.

Our simulations were performed on the $N = L_x \times L_y$ lattices with periodic boundary conditions imposed on the x and y directions. In this work, we mainly study four lattices of 6×6 , 10×10 , 12×10 , and 14×14 . The electron density is defined as $\langle n \rangle = N_e/N$, where N_e electrons are filled in the lattice with N sites. We take t as the energy unit and t' is varied from 0.02 to 1.0. The average number of random walkers is set to 2000 for $U \leq 2.0$ and 4000 for $2.0 < U \leq 4.0$. We performed 1280 Monte Carlo steps before measurements and did measurements in 20 blocks of 320 steps each to ensure statistical independence. $\Delta\tau$ in Eq. (2) was set to be 0.05.

To study the d -wave SC properties of the doped checkerboard Hubbard model, we compute the cluster [61] and conventional d -wave pairing correlations. The cluster (conventional) denotes hole pairing within the same 2×2 plaquette (between NN sites). The averages of long-range cluster and conventional d -wave pairing correlations are defined as

$$\bar{P}_{\text{cluster}}(R > 2) = \frac{1}{N_1} \sum_{|\vec{R}_m - \vec{R}_n| > 2} \langle \Delta_d^\dagger(\vec{R}_m) \Delta_d(\vec{R}_n) \rangle, \quad (3)$$

$$\bar{P}_{d\text{-wave}}(R > 2) = \frac{1}{N_2} \sum_{|\vec{r}_i - \vec{r}_j| > 2} \langle \Delta_d^\dagger(\vec{r}_i) \Delta_d(\vec{r}_j) \rangle, \quad (4)$$

where $\Delta_d^\dagger(\vec{R}_m)$ and $\Delta_d^\dagger(\vec{r}_i)$ [$\Delta_d(\vec{R}_n)$ and $\Delta_d(\vec{r}_j)$] are the electron pair creation (annihilation) operators. \vec{R}_m and \vec{R}_n correspond to the position vectors of the left bottom sites of plaquettes m and n . \vec{r}_i and \vec{r}_j represent the position vectors of lattice sites i and j . $N_1 = N/4 - 5$ and $N_2 = N - 13$ are the numbers of electron pairs with distances of $R > 2$. The cluster and conventional d -wave electron pair operators are given by

$$\Delta_d(\vec{R}_m) = \sum_{\vec{\delta}_0, \vec{\delta}} f(\vec{\delta}) (c_{\vec{R}_m + \vec{\delta}_0, \uparrow} c_{\vec{R}_m + \vec{\delta}, \downarrow} - c_{\vec{R}_m + \vec{\delta}_0, \downarrow} c_{\vec{R}_m + \vec{\delta}, \uparrow}), \quad (5)$$

$$\Delta_d(\vec{r}_i) = \sum_{\vec{\delta}'} f(\vec{\delta}') (c_{\vec{r}_i, \uparrow} c_{\vec{r}_i + \vec{\delta}', \downarrow} - c_{\vec{r}_i, \downarrow} c_{\vec{r}_i + \vec{\delta}', \uparrow}), \quad (6)$$

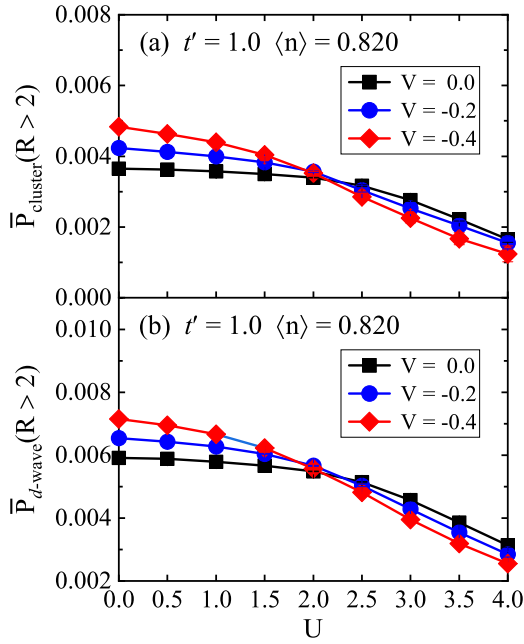


FIG. 2. The average of long-range d -wave pairing correlations $\bar{P}_{\text{cluster}}(R > 2)$ and $\bar{P}_{d\text{-wave}}(R > 2)$ as a function of U on the 10×10 lattice with $t' = 1.0$ at $V = 0.0, -0.2$, and -0.4 . (a) Cluster d -wave pairing correlation and (b) conventional d -wave pairing correlation.

where $f(\vec{\delta})$ and $f(\vec{\delta}')$ are the form factors of d -wave pairing symmetry with $f(\pm\vec{x}) = 1$, $f(\pm\vec{y}) = -1$. For $\Delta(\vec{R}_m)$, $\vec{\delta}_0 = 0$, $\vec{x} + \vec{y}$, $\vec{\delta} = \vec{x}, \vec{y}$. For $\Delta(\vec{r}_i)$, $\vec{\delta}' = \pm\vec{x}, \pm\vec{y}$. The cluster and conventional pairing patterns are illustrated in Figs. 1(b) and 1(c).

To promote understanding of the CPQMC results, we perform an ED study for the 2×2 plaquette. The pair binding energy (E_b) on the plaquette is defined by [62]

$$E_b = E(2, 2) + E(1, 1) - 2E(2, 1), \quad (7)$$

where $E(M_1, M_2)$ represents the ground energy of the isolated plaquette with M_1 spin-up and M_2 spin-down electrons. A negative E_b indicates that the plaquette favors hole pairing. Moreover, considering that the negative V might produce a phase separation (PS), we also compute the following energy difference:

$$E_{62-44} = E(3, 3) + E(1, 1) - 2E(2, 2). \quad (8)$$

A negative E_{62-44} implies that the half-filled plaquette with two spin-up and two spin-down electrons tends to phase separate into a two-hole rich phase and a two-electron rich phase.

III. RESULTS AND DISCUSSION

A. Homogeneous case: $t'/t = 1$

We first analyze the effect of intraplaquette NN attraction on the d -wave SC properties for the homogeneous case. Figure 2 shows the average of long-range d -wave pairing correlations as a function of U at $V = 0.0, -0.2$, and -0.4 on the 10×10 lattice with $t' = 1.0$. The electron density was chosen as $\langle n \rangle = 0.820$. One can clearly see that at $V = 0.0$, both $\bar{P}_{\text{cluster}}(R > 2)$ and $\bar{P}_{d\text{-wave}}(R > 2)$ monotonically

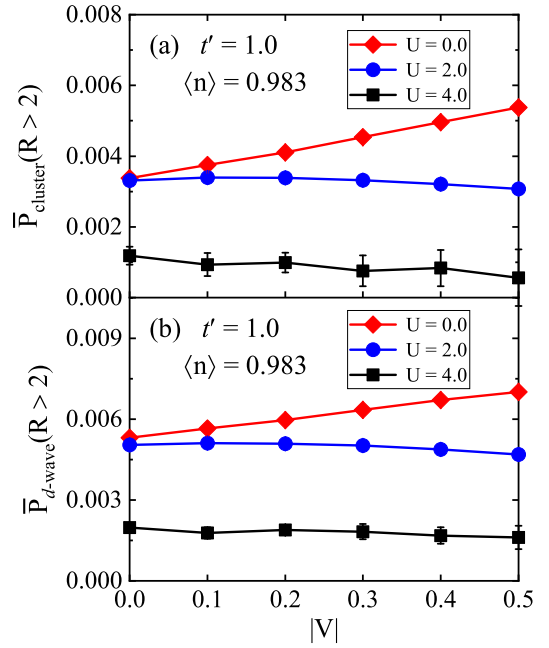


FIG. 3. The average of long-range d -wave pairing correlations as a function of $|V|$ on the 12×10 lattice with $t' = 1.0$ at $U = 0.0, 2.0$, and 4.0 . (a) Cluster d -wave pairing correlation and (b) conventional d -wave pairing correlation.

decrease with increasing U . In the ranges of $0.0 \leq U < 2.0$ and $2.0 < U \leq 4.0$, both $\bar{P}_{\text{cluster}}(R > 2)$ and $\bar{P}_{d\text{-wave}}(R > 2)$ exhibit a weak enhancement and suppression effect with the increase of $|V|$, respectively. For $U = 0.0$ and $U = 4.0$, the ratios between $\bar{P}_{\text{cluster}}(R > 2)$ at $V = -0.4$ and the ones at $V = 0.0$ are 1.32 and 0.75, respectively. To gain further insight into the role of NN attraction in the lightly hole-doped systems, in Fig. 3 we present the average of long-range d -wave pairing correlations as a function of $|V|$ at $U = 0.0, 2.0$, and 4.0 on the 12×10 lattice with $\langle n \rangle = 0.983$. Here, the checkerboard lattice was chosen as a rectangular lattice so that a wide range of closed-shell electron fillings, especially the ones close to half-filling, can be adopted for CPQMC simulations. One can readily see that both $\bar{P}_{\text{cluster}}(R > 2)$ and $\bar{P}_{d\text{-wave}}(R > 2)$ display a nearly linear increase with increasing $|V|$ at $U = 0.0$, while they are slightly suppressed by NN attraction at $U = 2.0$ and $U = 4.0$. The results shown in Figs. 2 and 3 provide a strong support for the presence of V -induced d -wave superconductivity in both half-filled [36,37] and doped [38] weakly correlated electron systems.

B. Inhomogeneous case: $t'/t < 1$

Now we turn to discuss the effect of intraplaquette NN attraction on the d -wave SC properties in the inhomogeneous case. Figure 4 shows the average of long-range d -wave pairing correlations as a function of U at $V = 0.0, -0.2$, and -0.4 on the 10×10 lattice with $t' = 0.05$ and $\langle n \rangle = 0.820$. The dashed line indicates the result of the free electron system with $U = 0.0$ and $V = 0.0$. Similar to the homogeneous case, both $\bar{P}_{\text{cluster}}(R > 2)$ and $\bar{P}_{d\text{-wave}}(R > 2)$ display a monotonic decrease with increasing U at $V = 0.0$. However, the effect of V on the long-range d -wave pairing correlations is

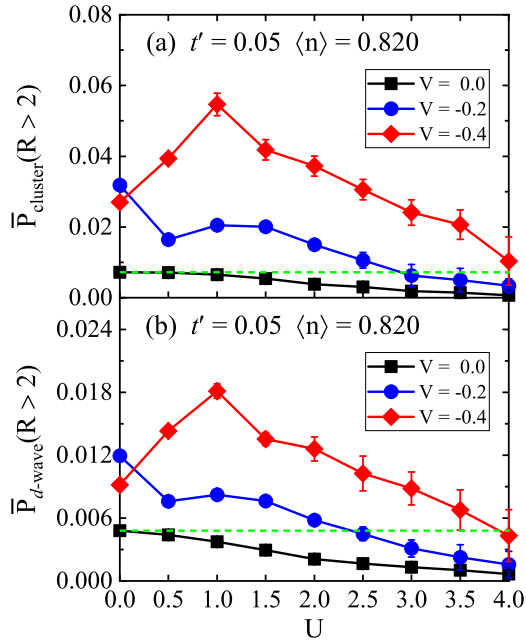


FIG. 4. The average of long-range d -wave pairing correlations as a function of U on the 10×10 lattice with $t' = 0.05$ at $V = 0.0, -0.2$, and -0.4 . (a) Cluster d -wave pairing correlation and (b) conventional d -wave pairing correlation.

distinct from the homogeneous case. As $|V|$ is increased, the long-range d -wave pairing correlations are dramatically enhanced, and the ratios between $\bar{P}_{\text{cluster}}(R > 2)$ at $V = -0.4$ and the ones at $V = 0.0$ are 8.41, 9.69, 13.17, and 14.58 for $U = 1.0, 2.0, 3.0$, and 4.0 , respectively, manifesting one order enhancement of d -wave pairing correlations. Remarkably, both $\bar{P}_{\text{cluster}}(R > 2)$ and $\bar{P}_{d\text{-wave}}(R > 2)$ at $V = -0.4$ exceed the values of free electron system, suggesting that d -wave superconductivity could be realized in the extended checkerboard Hubbard model.

A limited number of simulations for $t' = 0.05$ and $V = -0.2$ with V exerted on all NN sites show a similar enhancement of d -wave pairing correlations to the one presented in Fig. 4. These results demonstrate that the inhomogeneous hopping integral plays a crucial role in the V -induced enhancement of d -wave pairing correlations. Notice that, at $U = 0.0$, the enhancement of both $\bar{P}_{\text{cluster}}(R > 2)$ and $\bar{P}_{d\text{-wave}}(R > 2)$ is weaker at $V = -0.4$ than at $V = -0.2$, which will be attributed to the competition between V -induced pairing and PS (see Fig. 10).

We also examine the effect of NN attraction on both extended and on-site s -wave pairing channels. Figure 5(a) shows the average of long-range extended s -wave pairing correlations [$\bar{P}_{s\text{-wave}}(R > 2)$] as a function of U at $V = 0.0, -0.2$, and -0.4 , and a similar result for the on-site s -wave [$\bar{P}_{s\text{-wave}}(R > 2)$] is given in Fig. 5(b). The other parameters are the same as the ones in Fig. 4. Here, the two averages are obtained by replacing the pair operator $\Delta_d(\vec{r}_i)$ in Eq. (4) with $\Delta_s(\vec{r}_i) = c_{\vec{r}_i, \uparrow} c_{\vec{r}_i, \downarrow}$ and $\Delta_{s^*}(\vec{r}_i) = \sum_{\vec{\delta}} (c_{\vec{r}_i, \uparrow} c_{\vec{r}_i + \vec{\delta}, \downarrow} - c_{\vec{r}_i, \downarrow} c_{\vec{r}_i + \vec{\delta}, \uparrow})$, respectively. The results presented in Fig. 5 show that the extended s -wave pairing correlations take negative values and are hardly affected by

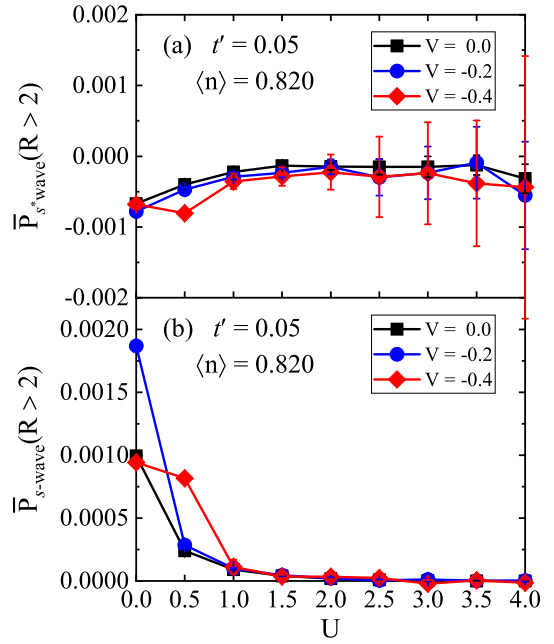


FIG. 5. The average of long-range s -wave pairing correlations as a function of U on the 10×10 lattice with $t' = 0.05$ at $V = 0.0, -0.2$, and -0.4 . (a) Extended s -wave pairing correlation and (b) on-site s -wave pairing correlation.

V , while the on-site s -wave pairing correlations exhibit an anomalous increase at $V = -0.2$ and $V = -0.4$ for $U = 0.0$ and $U = 0.5$, respectively, which can be attributed to the PS-induced enhancement of double occupancy (see Fig. 10). As $|V|$ is increased from 0.2 to 0.4, a sudden drop of $\bar{P}_{s\text{-wave}}(R > 2)$ occurs for $U = 0.0$. Nonetheless, one order of magnitude smaller s -wave pairing correlations compared to the d -wave ones suggest that d -wave pairing is dominant in the studied parameter regime. In Fig. 6, we investigate in more detail the effect of V on the d -wave pairing correlations for different t' . At $U = 0.5$, both $\bar{P}_{\text{cluster}}(R > 2)$ and $\bar{P}_{d\text{-wave}}(R > 2)$ exhibit a nonmonotonic dependence on V for $t' = 0.02, 0.05$, and 0.1 , as shown in Figs. 6(a) and 6(b). The d -wave pairing correlations first increase with increasing $|V|$ until $|V| = 0.3$ ($t' = 0.02$ and 0.05) and 0.4 ($t' = 0.1$), and then turn to decrease with further increasing $|V|$. For $t' = 0.2$, the d -wave pairing correlations show a monotonic increase with increasing $|V|$. At $U = 2.0$, the d -wave pairing correlations monotonically increase with increasing $|V|$ for $t' = 0.05$ and 0.1 , and exhibit a nonmonotonic behavior for $t' = 0.02$, as shown in Figs. 6(c) and 6(d). Another difference from $U = 0.5$ is that V has little effect on the d -wave pairing correlations for $t' = 0.2$. A comparison of the results in Fig. 6 reveals that the smaller is t' , the stronger is the V -induced enhancement effect.

Figure 7 displays $P_{\text{cluster}}(R)$ and $P_{d\text{-wave}}(R)$ as a function of pairing distance R at different V with $t' = 0.05$. The simulations were carried out on the 14×14 lattice and the electron density was chosen as $\langle n \rangle = 0.827$, which is close to the one for the 10×10 lattice. It is apparent that $P_{\text{cluster}}(R)$ and $P_{d\text{-wave}}(R)$ increase with increasing $|V|$ at all long-range pairing distances for both $U = 0.5$ and $U = 2.0$, and the en-

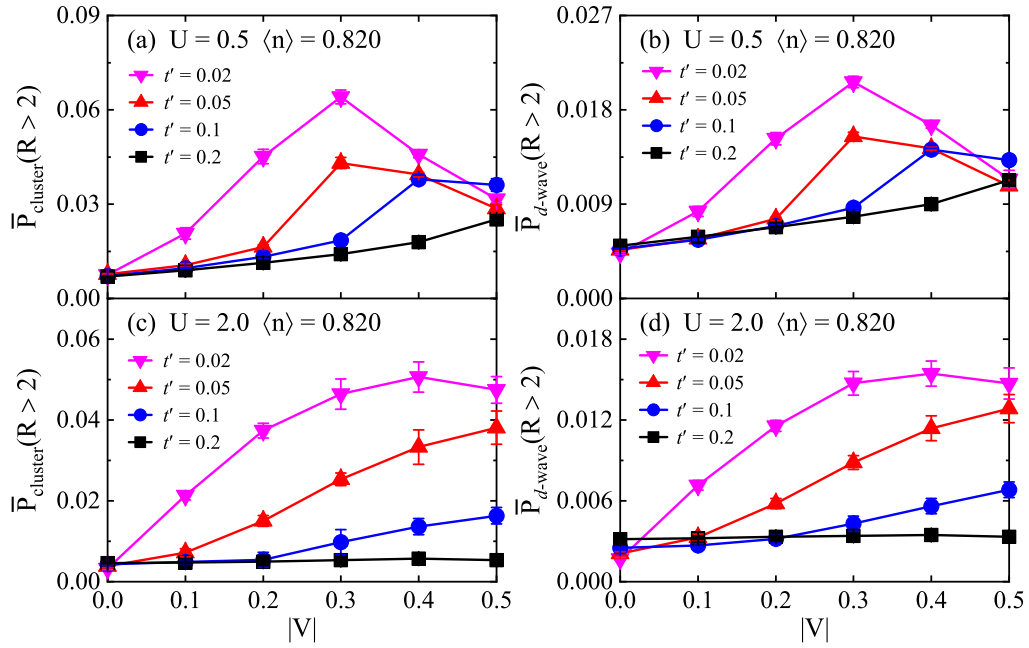


FIG. 6. The average of long-range d -wave pairing correlations as a function of $|V|$ on the 10×10 lattice with different t' . [(a),(b)] $U = 0.5$ and [(c),(d)] $U = 2.0$.

enhancement is much stronger at $V = -0.4$ than at $V = -0.2$. The results obtained on the larger lattice provide a strong support for the V -induced enhancement of d -wave superconductivity. Next, we investigate the checkerboard Hubbard model with different hole-doping densities δ ($\delta = 1 - \langle n \rangle$). Figure 8 presents $\bar{P}_{\text{cluster}}(R > 2)$ and $\bar{P}_{d\text{-wave}}(R > 2)$ as a function of δ at $U = 2.0$ and $t' = 0.05$ on the 12×10 lattice. One can readily see that, in the range of $0.05 < \delta < 0.45$, both $\bar{P}_{\text{cluster}}(R > 2)$ and $\bar{P}_{d\text{-wave}}(R > 2)$ are drastically enhanced by V . In contrast, the d -wave pairing correlations exhibit a weak

dependence on V as the hole-doping density approaches 0.0 or 0.5. When δ is close to 0.0 (corresponding to half filling), most of the 2×2 plaquettes lie in the half-filled state, making it difficult for a small number of hole pairs to form phase coherence. On the other hand, when δ is close to 0.5, each plaquette prefers two doped holes, forming a hardcore boson [47]. A previous study based on the hardcore boson model indicates that at half-filling, corresponding to $\delta = 0.5$ in our case, the hardcore boson is liable to form insulating state [63]. Therefore, despite the NN attraction V promotes the formation

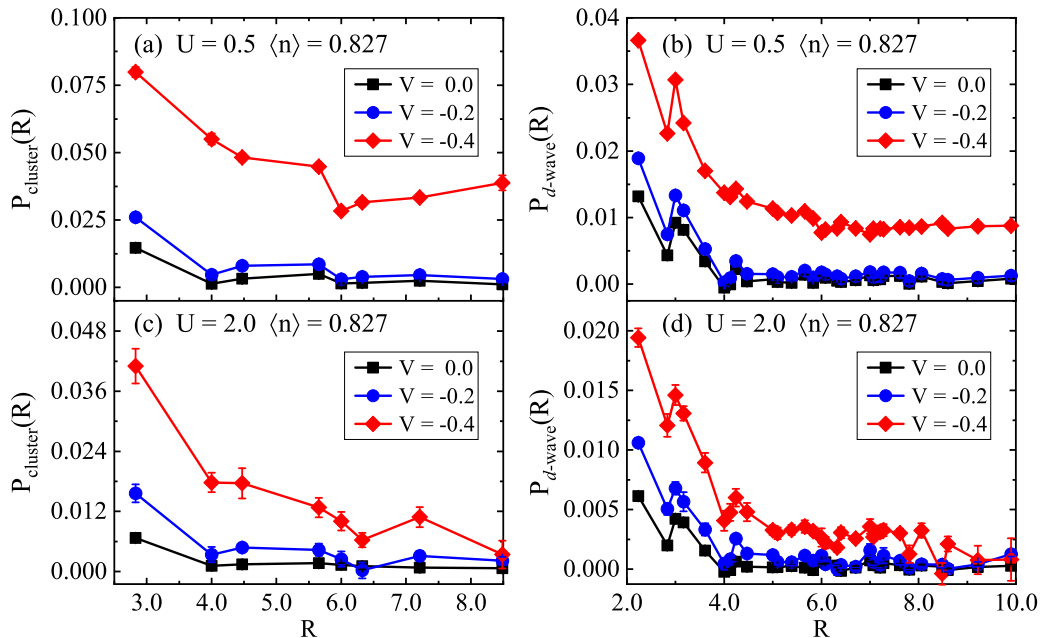


FIG. 7. The d -wave pairing correlations $P_{\text{cluster}}(R)$ and $P_{d\text{-wave}}(R)$ as a function of the distance R on the 14×14 lattice with $t' = 0.05$ at $V = 0.0, -0.2$, and -0.4 . [(a),(b)] $U = 0.5$ and [(c),(d)] $U = 2.0$.

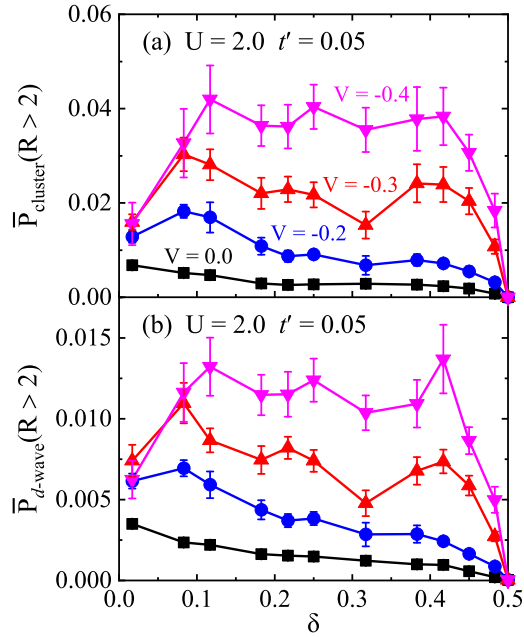


FIG. 8. The average of long-range d -wave pairing correlations as a function of δ on the 12×10 lattice with $t' = 0.05$ at $U = 2.0$ for different V . (a) Cluster d -wave pairing correlation and (b) conventional d -wave pairing correlation.

of hardcore boson, it does not effectively enhance d -wave superconductivity.

Figure 9 displays the average of long-range d -wave pairing correlations as a function of $|V|$ at $U = 0.0, 0.5$, and 1.0 on the 12×10 lattice with $\langle n \rangle = 0.983$. It is found that both

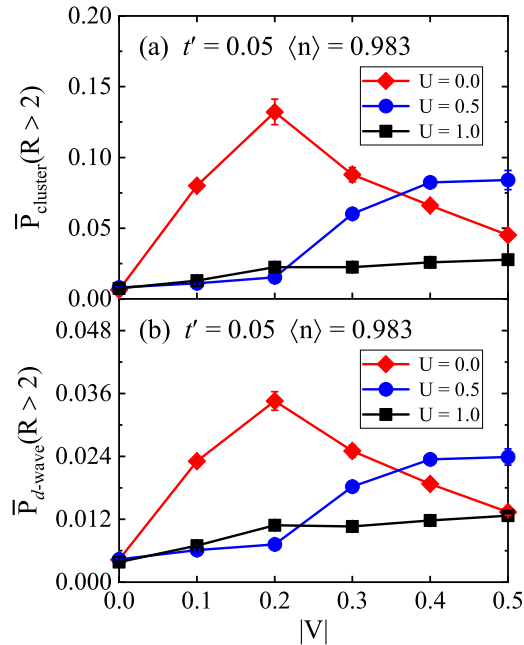


FIG. 9. The average of long-range d -wave pairing correlations as a function of $|V|$ on the 12×10 lattice with $t' = 0.05$ at $U = 0.0, 0.5$, and 1.0 . (a) Cluster d -wave pairing correlation and (b) conventional d -wave pairing correlation.

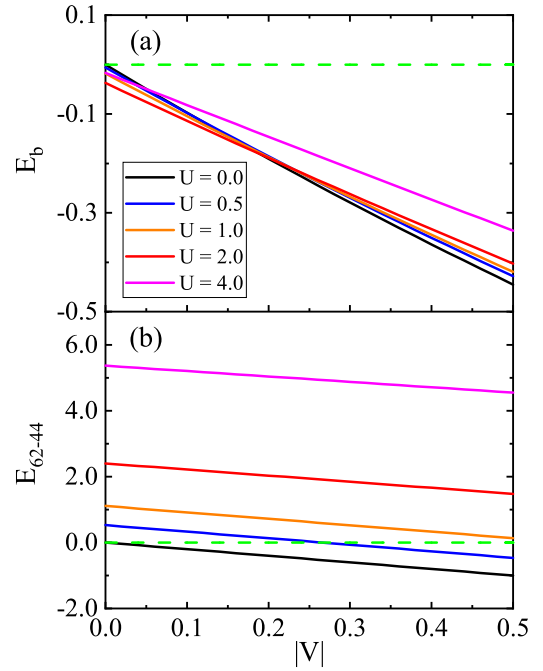


FIG. 10. (a) The electron pair binding energy E_b and (b) energy difference E_{62-44} as a function of $|V|$ at different U . The green dashed lines indicate the position of $E_b = 0.0$ or $E_{62-44} = 0.0$.

$\bar{P}_{\text{cluster}}(R > 2)$ and $\bar{P}_{d\text{-wave}}(R > 2)$ exhibit distinct V dependence at different Hubbard interactions: The d -wave pairing correlations at $U = 0.0$ first rapidly increase with increasing $|V|$ and begin to decrease when $|V|$ exceeds 0.2 ; The d -wave pairing correlations are slightly enhanced by NN attraction until $|V| = 0.2$, and then turn to rapidly increase and saturate with increasing $|V|$ further for $U = 0.5$ and $U = 1.0$, respectively. A comparison of the results presented in Figs. 3 and 9 indicates that, close to half-filling, the enhancement of d -wave superconductivity at $U = 0.0$ is one order of magnitude larger for the inhomogeneous case than for the homogeneous case.

C. ED results on the 2×2 plaquette and discussion

Finally, we try to understand the results of CPQMC using the ED method. In Fig. 10, we display the electron pair binding energy E_b on the 2×2 plaquette and the energy difference E_{62-44} as a function of $|V|$ at different U . At $V = 0.0$, E_b has a minimum $E_b^{\text{min}} = -0.039$ at $U = 2.46$. As seen from Fig. 10(a), E_b exhibits a monotonic decreasing dependence on $|V|$ for all U , and the decreasing rate is slightly reduced with increasing U . More negative E_b for larger $|V|$ indicates that the NN attraction is favorable to the formation of hole pairs in the studied parameter regime. Figure 10(b) shows that E_{62-44} decreases monotonically with increasing $|V|$ for all U and changes to negative value at a critical $V_c = 0.0$ for $U = 0.0$ and $V_c \sim -0.25$ for $U = 0.5$, respectively. This indicates that, in the parameter regime $U < 1.0$, PS starts at the critical V_c and becomes stronger as $|V|$ is increased.

Based on the ED results, the enhancement of pair binding energy is responsible for the enhancement of d -wave superconductivity in the parameter regime $U \geq 1.0$, while both hole pairing and PS are crucial for understanding the pairing

TABLE I. Comparison of the d -wave pairing correlations (D_{2d}) from the CPQMC simulations and exact results on the 4×4 lattice with $5\uparrow$ and $5\downarrow$ electrons at $U = 4.0$. The free electron wave function was used as the trial wave function in the CPQMC simulations, and the Monte Carlo errors are shown in parentheses.

	ED	CPQMC
$D_{2d}(2,1)$ ($t_1 = 0.00$)	0.02453	0.02455(9)
$D_{2d}(1,0)$ ($t_1 = 0.22$)	0.08655	0.0863(4)
$D_{2d}(1,1)$ ($t_1 = 0.22$)	-0.01403	-0.0144(2)
$D_{2d}(2,1)$ ($t_1 = 0.22$)	0.02339	0.0228(2)
$D_{2d}(2,2)$ ($t_1 = 0.22$)	0.13411	0.1304(5)

correlations in the parameter regime $U < 1.0$. In the lightly hole-doped case ($\langle n \rangle = 0.983$), where the hole pairing is of secondary importance, the results shown in Fig. 9 indicate that weak PS can induce a dramatic enhancement of d -wave superconductivity for $U = 0.0$ and $U = 0.5$, which is then suppressed by strong PS beyond a certain NN attraction. Such a dual role of PS was also observed in the homogeneous systems [41,64], and simultaneously, it causes the anomalous increase and drop of on-site s -wave pairing correlations as shown in Fig. 5, evidenced by very similar evolutions of $\bar{P}_{s\text{-wave}}(R > 2)$ with V to the ones in Fig. 9(b) for $U = 0.0$ and $U = 0.5$.

A combination of the results in Fig. 4 and Fig. 9 demonstrates that, when the hole pairing and PS have equal importance, there exists a strong competition between them, otherwise, the enhancement effect at $U = 0.0$ and $V = -0.2$ as well as at $U = 0.5$ and $V = -0.4$ should be stronger for $\langle n \rangle = 0.820$ than for $\langle n \rangle = 0.983$. Moreover, the competition between hole pairing and PS is manifested in the $U = 0.5$ and $t' = 0.05$ curves displayed in Figs. 6 and 9, which show opposite evolutions with increasing $|V|$ from 0.3 to 0.5. Furthermore, the competition between hole pairing and PS provides a reasonable explanation for the dip appearing at $U = 0.5$ in the $V = -0.2$ curves shown in Fig. 4. For the parameters $U = 0.5$ and $V = -0.2$, although the system lies in the uniform state, the tendency to PS could act to suppress the d -wave pairing correlations contributed by doped holes, leading to smaller $\bar{P}_{\text{cluster}}(R > 2)$ and $\bar{P}_{d\text{-wave}}(R > 2)$ compared to the ones at $U = 1.0$.

Our findings at small t' are consistent with the picture proposed by Kivelson *et al.* [47,49] in which the 2×2 plaquettes act as the centers of hole attraction, and then the interplaquette t' drives d -wave superconductivity in the two-dimensional lattice. The results presented in Appendix B indicate that this local pairing picture is applicable for larger Hubbard interactions ($U > 4.0$) in the parameter regime $t' < 0.2$. One question arising is how to realize local pairing in the homogeneous system. As pointed out by Tang and Hirsch [65], the Peierls instability can produce the same checkerboard hopping pattern on the square lattice as shown in Fig. 1(a), when electrons are coupled to two frozen phonons, one with a wave vector $(\pi, 0)$ and the other with a wave vector $(0, \pi)$. Therefore, it is expected that, in the homogeneous system with electrons coupled to dynamic $(\pi, 0)$ and $(0, \pi)$ phonons, dynamic checkerboard hopping (each bond alternating between

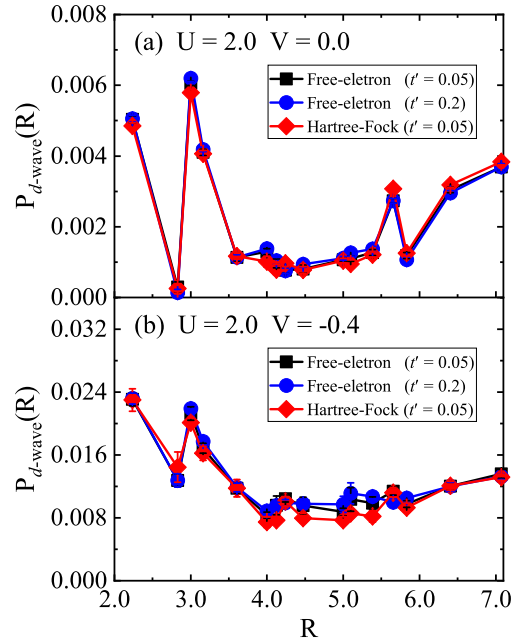


FIG. 11. The d -wave pairing correlation $P_{d\text{-wave}}(R)$ as a function of the distance R on the 10×10 checkerboard lattice with $t' = 0.05$ at $U = 2.0$ and $\langle n \rangle = 0.820$. Different trial wave functions are indicated by the symbols. (a) $V = 0.0$ and (b) $V = -0.4$.

solid and dashed lines) can promote the formation of d -wave superconductivity.

IV. CONCLUSION

In summary, we investigate the effect of intraplaquette NN attraction V on the d -wave SC property of the well-known two-dimensional checkerboard Hubbard model. The simulations reveal that, in the homogeneous system, V induces a significant enhancement of d -wave superconductivity near half-filling in the range of $0.0 \leq U < 2.0$; when the interplaquette hopping integral is small, V drastically enhances d -wave superconductivity in the studied range of $0.0 \leq U \leq 6.0$. For $t' = 0.05$, the long-range d -wave pairing correlations at $V = -0.4$ are approximately one order of magnitude larger than the ones at $V = 0.0$. The ED studies indicate that this enhancement effect originates from the V -induced enhancement of pair binding energy, and there exists a strong competition between hole pairing and PS in the weak correlation regime. Our findings not only deepen the understanding of the extended checkerboard Hubbard model, but also provide a promising route for the search of high-temperature superconductivity in the inhomogeneous correlated electron systems.

ACKNOWLEDGMENTS

We acknowledge helpful discussions with S.-Z. Zhou, X.-J. Zheng, and L. Du. This work was supported by the National Natural Science Foundation of China (Grant No. 11674087).

APPENDIX A: BENCHMARK OF THE CPQMC METHOD

Here we present the benchmark study for the CPQMC method. First, we compare the results for the uniform

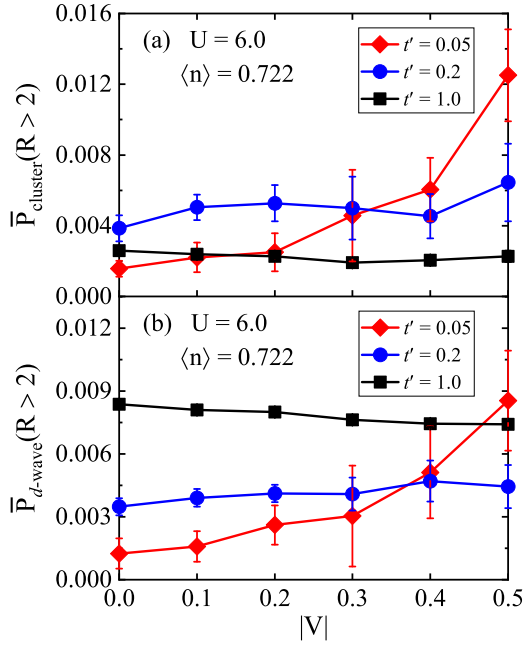


FIG. 12. The average of long-range d -wave pairing correlations as a function of $|V|$ on the 6×6 lattice with different t' . (a) Cluster d -wave pairing correlation and (b) conventional d -wave pairing correlation.

$t - t_1 - U$ Hubbard model obtained from the ED and CPQMC methods. The NN hopping integral t is taken as the energy unit and t_1 denotes the next NN hopping integral. Table I lists the d -wave pairing correlations (D_{2d}) on the 4×4 lattice with $5\uparrow$ and $5\downarrow$ electrons at $U = 4.0$. The ED results for $t_1 = 0.00$ and $t_1 = 0.22$ are from Refs. [58] and [66], respectively. The d -wave pairing correlation in this section is defined as [58]

$$D_{2d}(\vec{l}) = \langle \Delta_{2d}^\dagger(\vec{l}) \Delta_{2d}(\vec{0}) \rangle, \quad (\text{A1})$$

where $\vec{l} = (l_x, l_y)$ is the position vector of lattice site l and $\Delta_{2d}(\vec{l}) = \sum_{\vec{\delta}} f(\vec{\delta}) c_{l+\vec{\delta},\uparrow}^\dagger c_{l,\downarrow}$ denotes the d -wave pair operator, which is different from the one in Eq. (6). From

Table I, one can clearly see that the CPQMC data are in excellent agreement with the ED results, with relative deviations from the ED results being less than 3.0%.

In Fig. 11, we compare $P_{d\text{-wave}}(R)$ on the 10×10 checkerboard lattice with $t' = 0.05$ at $U = 2.0$ and $\langle n \rangle = 0.820$ obtained from different trial wave functions. Two free-electron wave functions, one with $t' = 0.05$ and the other with $t' = 0.2$, as well as a Hartree-Fock mean-field wave function, were used as the trial wave functions. The Hartree-Fock wave function was obtained by diagonalizing the following quadratic Hamiltonian

$$H^{HF} = -t \sum_{\langle i,j \rangle, \sigma} (c_{i,\sigma}^\dagger c_{j,\sigma} + \text{H.c.}) - t' \sum_{\langle ij \rangle', \sigma} (c_{i,\sigma}^\dagger c_{j,\sigma} + \text{H.c.}) + U \sum_i (\langle n_{i,\uparrow} \rangle n_{i,\downarrow} + \langle n_{i,\downarrow} \rangle n_{i,\uparrow} - \langle n_{i,\uparrow} \rangle \langle n_{i,\downarrow} \rangle). \quad (\text{A2})$$

where $\langle n_{i,\uparrow} \rangle$ and $\langle n_{i,\downarrow} \rangle$ stand for the mean fields of spin-up and spin-down electrons. As seen from Fig. 11, the d -wave pairing correlations obtained from the three trial wave functions are in agreement with each other at all distances, and the agreement is better for $V = 0.0$ than for $V = -0.4$. The results shown in Fig. 11 demonstrate that the physical observables are insensitive to the choice of trial wave function.

APPENDIX B: CPQMC RESULTS ON THE 6×6 LATTICE FOR $U = 6.0$

In this Appendix, we examine whether the V -induced drastic enhancement of d -wave superconductivity is applicable for larger U . Figure 12 displays the average of long-range d -wave pairing correlations as a function of $|V|$ at $t' = 0.05, 0.2$, and 1.0 on the 6×6 lattice with $U = 6.0$ and $\langle n \rangle = 0.722$. At $t' = 0.2$ and 1.0 , both $\bar{P}_{\text{cluster}}(R > 2)$ and $\bar{P}_{d\text{-wave}}(R > 2)$ are weakly dependent on $|V|$ and exhibit a tendency to be enhanced and suppressed by NN attraction for $t' = 0.2$ and 1.0 , respectively. In contrast, one order enhancement of d -wave pairing correlations is observed for $t' = 0.05$ with increasing $|V|$ from 0.0 to 0.5. The results presented in Fig. 12 suggest that our findings can be extended to the strong correlation regime.

-
- [1] J. G. Bednorz and K. A. Müller, Possible high T_c superconductivity in the Ba-La-Cu-O system, *Z. Phys. B: Condens. Matter* **64**, 189 (1986).
- [2] P. W. Anderson, The resonating valence bond state in La_2CuO_4 and superconductivity, *Science* **235**, 1196 (1987).
- [3] B. Keimer, S. A. Kivelson, M. R. Norman, S. Uchida, and J. Zaanen, From quantum matter to high-temperature superconductivity in copper oxides, *Nature (London)* **518**, 179 (2015).
- [4] K. Jiang, X. Wu, J. Hu, and Z. Wang, Nodeless High- T_c Superconductivity in the Highly Overdoped CuO_2 Monolayer, *Phys. Rev. Lett.* **121**, 227002 (2018).
- [5] N. P. Armitage, P. Fournier, and R. L. Greene, Progress and perspectives on electron-doped cuprates, *Rev. Mod. Phys.* **82**, 2421 (2010).
- [6] X. Zhou, W.-S. Lee, M. Imada, N. Trivedi, P. Phillips, H.-Y. Kee, P. Törmä, and M. Eremets, High-temperature superconductivity, *Nat. Rev. Phys.* **3**, 462 (2021).
- [7] C. Chu, L. Deng, and B. Lv, Hole-doped cuprate high temperature superconductors, *Phys. C: Supercond. Appl.* **514**, 290 (2015).
- [8] P. A. Lee, N. Nagaosa, and X.-G. Wen, Doping a Mott insulator: Physics of high-temperature superconductivity, *Rev. Mod. Phys.* **78**, 17 (2006).
- [9] T. M. Rice, K.-Y. Yang, and F. C. Zhang, A phenomenological theory of the anomalous pseudogap phase in underdoped cuprates, *Rep. Prog. Phys.* **75**, 016502 (2012).
- [10] Z.-X. Shen, D. S. Dessau, B. O. Wells, D. M. King, W. E. Spicer, A. J. Arko, D. Marshall, L. W. Lombardo, A. Kapitulnik, P. Dickinson, S. Doniach, J. DiCarlo, A. G. Loeser, and C. H. Park, Anomalously large gap anisotropy in the a - b plane of $\text{Bi}_2\text{Sr}_2\text{CaCu}_2\text{O}_{8+\delta}$, *Phys. Rev. Lett.* **70**, 1553 (1993).
- [11] C. C. Tsuei and J. R. Kirtley, Pairing symmetry in cuprate superconductors, *Rev. Mod. Phys.* **72**, 969 (2000).

- [12] S. H. Pan, J. O'neal, R. Badzey, C. Chamon, H. Ding, J. Engelbrecht, Z. Wang, H. Eisaki, S.-i. Uchida, A. Gupta *et al.*, Microscopic electronic inhomogeneity in the high- T_c superconductor $\text{Bi}_2\text{Sr}_2\text{CaCu}_2\text{O}_{8+x}$, *Nature (London)* **413**, 282 (2001).
- [13] H. Fong, P. Bourges, Y. Sidis, L. Regnault, A. Ivanov, G. Gu, N. Koshizuka, and B. Keimer, Neutron scattering from magnetic excitations in $\text{Bi}_2\text{Sr}_2\text{CaCu}_2\text{O}_{8+\delta}$, *Nature (London)* **398**, 588 (1999).
- [14] C. J. Halboth and W. Metzner, d -wave superconductivity and pomeranchuk instability in the two-dimensional hubbard model, *Phys. Rev. Lett.* **85**, 5162 (2000).
- [15] D. J. Scalapino, A common thread: The pairing interaction for unconventional superconductors, *Rev. Mod. Phys.* **84**, 1383 (2012).
- [16] B. M. Andersen, S. Graser, and P. J. Hirschfeld, Disorder-induced freezing of dynamical spin fluctuations in underdoped cuprate superconductors, *Phys. Rev. Lett.* **105**, 147002 (2010).
- [17] T. A. Maier, M. Jarrell, T. C. Schulthess, P. R. C. Kent, and J. B. White, Systematic Study of d -Wave superconductivity in the 2D repulsive hubbard model, *Phys. Rev. Lett.* **95**, 237001 (2005).
- [18] D. Sénéchal, P.-L. Lavertu, M.-A. Marois, and A.-M. S. Tremblay, Competition between antiferromagnetism and superconductivity in high- T_c cuprates, *Phys. Rev. Lett.* **94**, 156404 (2005).
- [19] H.-C. Jiang and T. P. Devereaux, Superconductivity in the doped Hubbard model and its interplay with next-nearest hopping t' , *Science* **365**, 1424 (2019).
- [20] S. Sakai, M. Civelli, and M. Imada, Hidden fermionic excitation boosting high-temperature superconductivity in cuprates, *Phys. Rev. Lett.* **116**, 057003 (2016).
- [21] K. Kuroki and H. Aoki, Quantum monte carlo evidence for superconductivity in the three-band hubbard model in two dimensions, *Phys. Rev. Lett.* **76**, 4400 (1996).
- [22] P. Corboz, T. M. Rice, and M. Troyer, Competing states in the t - J model: Uniform d -wave state versus stripe state, *Phys. Rev. Lett.* **113**, 046402 (2014).
- [23] M. Guerrero, J. E. Gubernatis, and S. Zhang, Quantum Monte Carlo study of hole binding and pairing correlations in the three-band Hubbard model, *Phys. Rev. B* **57**, 11980 (1998).
- [24] Z. B. Huang, H. Q. Lin, and E. Arrigoni, Strong enhancement of d -wave superconducting state in the three-band Hubbard model coupled to an apical oxygen phonon, *Phys. Rev. B* **83**, 064521 (2011).
- [25] M. Tsuchiizu, Y. Yamakawa, and H. Kontani, p -orbital density wave with d symmetry in high- T_c cuprate superconductors predicted by renormalization-group + constrained RPA theory, *Phys. Rev. B* **93**, 155148 (2016).
- [26] S. Raghu, S. A. Kivelson, and D. J. Scalapino, Superconductivity in the repulsive Hubbard model: An asymptotically exact weak-coupling solution, *Phys. Rev. B* **81**, 224505 (2010).
- [27] W. Cho, R. Thomale, S. Raghu, and S. A. Kivelson, Band structure effects on the superconductivity in Hubbard models, *Phys. Rev. B* **88**, 064505 (2013).
- [28] E. Gull and A. J. Millis, Superconducting and pseudogap effects on the interplane conductivity and Raman scattering cross section in the two-dimensional Hubbard model, *Phys. Rev. B* **88**, 075127 (2013).
- [29] S. Bulut, W. A. Atkinson, and A. P. Kampf, Spatially modulated electronic nematicity in the three-band model of cuprate superconductors, *Phys. Rev. B* **88**, 155132 (2013).
- [30] F. F. Assaad, M. Imada, and D. J. Scalapino, Quantum transition between an antiferromagnetic mott insulator and $d_{x^2-y^2}$ superconductor in two dimensions, *Phys. Rev. Lett.* **77**, 4592 (1996).
- [31] M. Vojta and S. Sachdev, Charge order, superconductivity, and a global phase diagram of doped antiferromagnets, *Phys. Rev. Lett.* **83**, 3916 (1999).
- [32] Z. Chen, Y. Wang, S. N. Rebec, T. Jia, M. Hashimoto, D. Lu, B. Moritz, R. G. Moore, T. P. Devereaux, and Z.-X. Shen, Anomalous strong near-neighbor attraction in doped 1D cuprate chains, *Science* **373**, 1235 (2021).
- [33] Y. Wang, Z. Chen, T. Shi, B. Moritz, Z.-X. Shen, and T. P. Devereaux, Phonon-mediated long-range attractive interaction in one-dimensional cuprates, *Phys. Rev. Lett.* **127**, 197003 (2021).
- [34] Z. B. Huang, W. Hanke, E. Arrigoni, and D. J. Scalapino, Electron-phonon vertex in the two-dimensional one-band Hubbard model, *Phys. Rev. B* **68**, 220507(R) (2003).
- [35] R. Micnas, J. Ranninger, S. Robaszkiewicz, and S. Tabor, Superconductivity in a narrow-band system with intersite electron pairing in two dimensions: A mean-field study, *Phys. Rev. B* **37**, 9410 (1988).
- [36] E. Dagotto, J. Riera, Y. C. Chen, A. Moreo, A. Nazarenko, F. Alcaraz, and F. Ortolani, Superconductivity near phase separation in models of correlated electrons, *Phys. Rev. B* **49**, 3548 (1994).
- [37] S. d. A. Sousa-Júnior, N. C. Costa, and R. R. D. Santos, Phase diagram for the extended Hubbard model on a square lattice, [arXiv:2304.08683](https://arxiv.org/abs/2304.08683).
- [38] S. Kundu and D. Sénéchal, CDMFT + HFD: an extension of dynamical mean field theory for nonlocal interactions applied to the single band extended Hubbard model, [arXiv:2310.16075](https://arxiv.org/abs/2310.16075).
- [39] C. Peng, Y. Wang, J. Wen, Y. S. Lee, T. P. Devereaux, and H.-C. Jiang, Enhanced superconductivity by near-neighbor attraction in the doped extended Hubbard model, *Phys. Rev. B* **107**, L201102 (2023).
- [40] M. Jiang, Enhancing d -wave superconductivity with nearest-neighbor attraction in the extended Hubbard model, *Phys. Rev. B* **105**, 024510 (2022).
- [41] A. Nazarenko, A. Moreo, E. Dagotto, and J. Riera, $d_{x^2-y^2}$ superconductivity in a model of correlated fermions, *Phys. Rev. B* **54**, R768(R) (1996).
- [42] R. Micnas, J. Ranninger, and S. Robaszkiewicz, Superconductivity in narrow-band systems with local nonretarded attractive interactions, *Rev. Mod. Phys.* **62**, 113 (1990).
- [43] L. Zhang, T. Guo, Y. Mou, Q. Chen, and T. Ma, Enhancement of d -wave pairing in the striped phase with nearest neighbor attraction, *Phys. Rev. B* **105**, 155154 (2022).
- [44] N. Plonka, C. J. Jia, Y. Wang, B. Moritz, and T. P. Devereaux, Fidelity study of superconductivity in extended Hubbard models, *Phys. Rev. B* **92**, 024503 (2015).
- [45] D.-W. Qu, B.-B. Chen, H.-C. Jiang, Y. Wang, and W. Li, Spin-triplet pairing induced by near-neighbor attraction in the extended Hubbard model for cuprate chain, *Commun. Phys.* **5**, 257 (2022).
- [46] Z. B. Huang, H. Q. Lin, and J. E. Gubernatis, Quantum monte carlo study of spin, charge, and pairing correlations in the $t - t' - U$ hubbard model, *Phys. Rev. B* **64**, 205101 (2001).

- [47] H. Yao, W.-F. Tsai, and S. A. Kivelson, Myriad phases of the checkerboard Hubbard model, *Phys. Rev. B* **76**, 161104(R) (2007).
- [48] W.-F. Tsai, H. Yao, A. Läuchli, and S. A. Kivelson, Optimal inhomogeneity for superconductivity: Finite-size studies, *Phys. Rev. B* **77**, 214502 (2008).
- [49] W.-F. Tsai and S. A. Kivelson, Superconductivity in inhomogeneous Hubbard models, *Phys. Rev. B* **73**, 214510 (2006).
- [50] G. Karakostas, E. Berg, S. R. White, and S. A. Kivelson, Enhanced pairing in the checkerboard Hubbard ladder, *Phys. Rev. B* **83**, 054508 (2011).
- [51] S. Baruch and D. Orgad, Contractor-renormalization study of Hubbard plaquette clusters, *Phys. Rev. B* **82**, 134537 (2010).
- [52] G. Wachtel, S. Baruch, and D. Orgad, Optimal inhomogeneity for pairing in Hubbard systems with next-nearest-neighbor hopping, *Phys. Rev. B* **96**, 064527 (2017).
- [53] D. G. S. P. Doluweera, A. Macridin, T. A. Maier, M. Jarrell, and T. Pruschke, Suppression of d -wave superconductivity in the checkerboard Hubbard model, *Phys. Rev. B* **78**, 020504(R) (2008).
- [54] S. Chakraborty, D. Sénéchal, and A.-M. S. Tremblay, d -wave superconductivity on the checkerboard Hubbard model at weak and strong coupling, *Phys. Rev. B* **84**, 054545 (2011).
- [55] T. Ying, R. Mondaini, X. D. Sun, T. Paiva, R. M. Fye, and R. T. Scalettar, Determinant quantum Monte Carlo study of d -wave pairing in the plaquette Hubbard hamiltonian, *Phys. Rev. B* **90**, 075121 (2014).
- [56] P. Kumar, T. I. Vanhala, and P. Törmä, Magnetization, d -wave superconductivity, and non-Fermi-liquid behavior in a crossover from dispersive to flat bands, *Phys. Rev. B* **100**, 125141 (2019).
- [57] S. Zhang, J. Carlson, and J. E. Gubernatis, Constrained path quantum monte carlo method for fermion ground states, *Phys. Rev. Lett.* **74**, 3652 (1995).
- [58] S. Zhang, J. Carlson, and J. E. Gubernatis, Constrained path Monte Carlo method for fermion ground states, *Phys. Rev. B* **55**, 7464 (1997).
- [59] J. Carlson, J. E. Gubernatis, G. Ortiz, and S. Zhang, Issues and observations on applications of the constrained-path Monte Carlo method to many-fermion systems, *Phys. Rev. B* **59**, 12788 (1999).
- [60] M. Qin, H. Shi, and S. Zhang, Benchmark study of the two-dimensional Hubbard model with auxiliary-field quantum Monte Carlo method, *Phys. Rev. B* **94**, 085103 (2016).
- [61] Y. Wu, S. Fang, G. Liu, and Y. Zhang, Possible cluster pairing correlation in the checkerboard Hubbard model: a quantum Monte Carlo study, *J. Phys.: Condens. Matter* **31**, 375601 (2019).
- [62] A. N. Kocharian, G. W. Fernando, K. Palandage, and J. W. Davenport, Exact study of charge-spin separation, pairing fluctuations, and pseudogaps in four-site Hubbard clusters, *Phys. Rev. B* **74**, 024511 (2006).
- [63] F. Hébert, G. G. Batrouni, R. T. Scalettar, G. Schmid, M. Troyer, and A. Dorneich, Quantum phase transitions in the two-dimensional hardcore boson model, *Phys. Rev. B* **65**, 014513 (2001).
- [64] E. Dagotto, Correlated electrons in high-temperature superconductors, *Rev. Mod. Phys.* **66**, 763 (1994).
- [65] S. Tang and J. E. Hirsch, Peierls instability in the two-dimensional half-filled Hubbard model, *Phys. Rev. B* **37**, 9546 (1988).
- [66] T. Husslein, W. Fettes, and I. Morgenstern, Comparison of calculations for the hubbard model obtained with quantum-monte-carlo, exact, and stochastic diagonalization, *Int. J. Mod. Phys. C* **08**, 397 (1997).